Regenerative Therapy 26 (2024) 783–791

Contents lists available at ScienceDirect

Regenerative Therapy

journal homepage: http://www.elsevier.com/locate/reth

Original Article

Generation of insulin-like growth factor 1 receptor-knockout pigs as a potential system for interspecies organogenesis

Masaki Nagaya [a, *], Ayuko Uchikura [a], Kazuaki Nakano [a, c], Masahito Watanabe [a, c], Hitomi Matsunari [a, c], Kazuhiro Umeyama [a, c], Naoaki Mizuno [d, e], Toshiya Nishimura [f], Hiromitsu Nakauchi [d, e, f], Hiroshi Nagashima [a, b, c, **]

[a] Meiji University International Institute for Bio-Resource Research, 1-1-1 Higashimita, Tama-ku, Kawasaki 214-8571, Japan
[b] Laboratory of Developmental Engineering, Department of Life Sciences, School of Agriculture, Meiji University, 1-1-1 Higashimita, Tama-ku, Kawasaki 214-8571, Japan
[c] PorMedTec Co. Ltd., 2-3227 Mita, Tama-ku, Kawasaki, Kanagawa, 214-0034, Japan
[d] Division of Stem Cell Therapy, Institute of Medical Science, University of Tokyo, Tokyo 108-8639, Japan
[e] Stem Cell Therapy Laboratory, Tokyo Medical and Dental University, 1-5-45 Yushima, Bunkyo-ku, 113-8510 Tokyo, Japan
[f] Institute for Stem Cell Biology and Regenerative Medicine, Stanford University School of Medicine, Stanford, CA94305, USA

ARTICLE INFO

Article history:
Received 30 July 2024
Received in revised form
27 August 2024
Accepted 29 August 2024

Keywords:
Insulin-like growth factor 1 receptor
Growth retardation
Pig
Blastocyst complementation techniques

ABSTRACT

Background: To overcome organ shortage during transplantation, interspecies organ generation via blastocyst complementation has been proposed, although not yet in evolutionarily distant species. To establish high levels of chimerism, low chimerism is required early in development, followed by high chimerism, to effectively complement the organ niche. Very few human cells are expected to contribute to chimerism in heterologous animals. Previous studies had demonstrated increased donor chimerism in both intra- and interspecies chimeras in rodents, using *insulin-like growth factor 1 receptor* (*Igf1r*) knockout (KO) mice; deletion of the *Igf1r* gene in the mouse host embryo created a cell-competitive niche. The current study aimed to generate *IGF1R*–KO pigs and evaluate whether they have the same phenotype as *Igf1r*-KO mice.
Methods: To generate *IGF1R*–KO pigs, genome-editing molecules were injected into the cytoplasm of pig zygotes. The fetuses were evaluated at 104 days of gestation.
Results: *IGF1R*–KO pigs were generated successfully. Their phenotypes were almost identical to those of *Igf1r*-KO mice, including small lungs and enlarged endodermal organs in fetuses, and they were highly reproducible.
Conclusions: Pigs may allow the generation of organs using blastocyst complementation with developmentally-compatible xenogeneic pluripotent stem cells over a large evolutionary distance.

1. Introduction

The problem of organ shortages during transplantation is a consistent challenge. Organ production using stem cell technology has been limited to the induction of tissue-specific cells [1] and organoids [2]; it does not produce functional organs. For producing functional organs, attempts have been made to generate fully-functional, heterologous organs *in vivo* from pluripotent stem cells (PSCs) using blastocyst complementation and exploitation of the developmental organ niche [3–6]. Mammals have master regulator genes that control the formation of tissues and organs [7–10], and knockout (KO) of such genes

Abbreviations: IGF1, Insulin-like growth factor 1; IGF1R, Insulin-like growth factor 1 receptor; CRISPR/Cas9, Clustered regularly interspaced short palindromic repeat-associated protein 9; gRNA, guide RNA; KO, knock-out; WT, wild-type; SEM, standard error of mean; GH, Growth hormone; RPKM, Reads per kilobase million.

* Corresponding author. Meiji University International Institute for Bio-Resource Research, 1-1-1 Higashimita Tama-ku Kawasaki, Kanagawa 214-8571, Japan.
** Corresponding author. Laboratory of Medical Bioengineering, Department of Life Sciences, School of Agriculture, Meiji University, 1-1-1 Higashimita Tama-ku Kawasaki, Kanagawa 214-8571, Japan.
E-mail addresses: m2nagaya@meiji.ac.jp (M. Nagaya), hnagas@meiji.ac.jp (H. Nagashima).

Peer review under responsibility of the Japanese Society for Regenerative Medicine.

https://doi.org/10.1016/j.reth.2024.08.025

results in individuals with phenotypes that lack specific tissues and organs. Studies on rodents have demonstrated that KO of *Pancreatic and duodenal homeobox 1(Pdx1), Spalt like transcription factor 1 (Sall1)*, and *Forkhead box protein N1(Foxn1)*, which induces a phenotype with hypoplasia or complete loss of the pancreas, kidney, and thymus, respectively [11–13]. *Kobayashi* et al. [5] and *Usui* et al. [14] successfully generated rat pancreas and kidneys *in vivo* in *Pdx1*-KO and *Sall1*-KO mice, respectively, using the blastocyst complementation approach. We extended this proof of concept to large animals and showed that homologous but missing organs can be complemented using blastocyst complementation techniques [15]. Techniques that exploit the void developmental niche in animals can also be applied to human organogenesis. Currently, human organs are not produced in other animal species, even using blastocyst complementation techniques. Despite human cells being viable in the animal tissues of a heterologous species, very few human cells would contribute to chimerism [16], leaving insufficient cells to complement the developmental niche for interspecies chimerism [3]. Functional human organs for transplantation cannot be generated unless the contribution of human donor cells increases in recipient animals that are heterologous to humans. Regional and temporal developmental problems occur during the generation of interspecies embryos. Heterologous cells may heterogeneously contribute to different lineages, resulting in regions with low chimerism [17]. Blastocyst complementation with many donor cells to compensate for regions of low chimerism does not improve overall chimerism. In evolutionarily diverse species, a high contribution of heterologous cells in the early developmental stages is associated with aberrations and embryonic lethality. To avoid such a lethal situation and establish chimerism, low chimerism during early development is required, followed by high chimerism to effectively complement the organ niche [18,19].

Insulin-like growth factor 1 (Igf1) is an important mediator of mammalian pre- and postnatal growth [20–22]; *Igf1* acts through the *Igf1 receptor (Igf1r)*, which is ubiquitously expressed in tissues and regulates mitogenic, anti-apoptotic, and transforming pathways [23]. Defects in the *Igf1r* gene in mouse embryos can cause growth retardation and neonatal death [21,22]. However, *Nishimura* et al. used a mouse model to demonstrate increased donor chimerism in both intra- and interspecies chimerism in rodents [18]. Deletion of *Igf1r* in the mouse host embryo creates a 'cell-competitive niche.' Importantly, *Igf1r* deletion opens the niche at a later stage of development than the early developmental arrest observed in interspecies, highly-chimeric embryos. Donor cells that persist until the niche opens can proliferate within the niche, facilitating *in vivo* organogenesis in distantly-related interspecies chimeras. These are crucial for organ production in human–pig chimeras. The current study aimed to generate *IGF1R*–KO pigs and assess whether they exhibit the same phenotype as *Igf1r*-KO mice and could be potential recipients for human–pig organogenesis.

2. Materials and methods

2.1. Animal care and chemicals

All animal experiments, including the genetic modifications performed in this study, were approved by the Institutional Animal Care and Use Committee (IACUC) of Meiji University (MUIACUC2022-07). All experiments were performed in accordance with the relevant guidelines and regulations. All chemicals were purchased from Sigma-Aldrich (St. Louis, MO, USA) unless indicated otherwise.

2.2. Design and preparation of porcine IGF1R-targeting guide RNA

Target sequences to knock out porcine *IGF1R* were designed using an online.

CRISPR design tool, CRISPOR (http://crispor.tefor.net/). Sequences without the adjacent protospacer motif are shown in Supplementary Table 1. The crispr RNA (crRNA) and transactivating crRNA (tracrRNA) for the preparation of guide RNA (gRNA) were obtained from Integrated DNA Technologies (Coralville, IA, USA). To form a ribonucleoprotein (RNP) complex, Cas9 protein (Takara Bio, Shiga, Japan) and gRNA (1:1 crRNA–tracrRNA duplex) were premixed. The RNP complex was freshly prepared immediately before the experiments and stored on ice until use.

2.3. Evaluation of each IGF1R-targeting guide RNA

To evaluate the genome-targeting efficiency of each designed gRNA, a nuclease-based mutation detection assay was performed using the Guide-it Mutation Detection Kit (Takara Bio) following the manufacturer's protocol. Briefly, the RNP complex was electroporated into porcine fetal fibroblasts, as described previously [24]. The cells were harvested after 48 h of electroporation and genomic DNA was extracted using the DNeasy Blood and Tissue Kit (QIAGEN). The target region of clustered, regularly-interspaced, short palindromic repeat-associated protein 9 (CRISPR-Cas9) was amplified using polymerase chain reaction (PCR) using the appropriate primers (see Section 2.7). The intensity ratio of cut to uncut bands on the agarose gel was analyzed using Image J software (National Institutes of Health, Bethesda, MD, USA), and the percentage of nuclease-specific cleavage products (fraction cleaved) was determined. The estimated gene modifications were calculated using the following formula:

$$\%\ \text{gene targeting efficiency} = 100 \times (1 - (1 - \text{fraction cleaved})^{1/2})$$

2.4. Preparation of pronuclear-stage embryos for cytoplasmic injection

Induction of parthenogenesis and in vitro fertilization (IVF) of porcine oocytes obtained by in vitro maturation (IVM) was performed as described previously [24]. For parthenogenetic activation, oocytes were washed twice in an activation solution composed of 280 mM mannitol (Nacalai Tesque, Inc., Kyoto, Japan), 0.05 mM $CaCl_2$, 0.1 mM $MgSO_4$, and 0.01% (w/v) polyvinyl alcohol. They were then aligned between two wire electrodes (1.0 mm apart) in a drop of activation solution on a fusion chamber slide (CUY500G1, Nepa Gene, Chiba, Japan). A single direct current pulse of 150 V/mm was applied for 100 μs using an electrical pulsing machine (LF201; Nepa Gene). The activated oocytes were treated with 5 μg/ml cytochalasin B for 3 h to suppress extrusion of the second polar body.

For IVF, frozen epididymal sperm (1.0×10^9/300 μl) from a WT boar were suspended in 5 ml of Dulbecco's phosphate-buffered saline (DPBS; Nissui Pharmaceutical Co., Ltd., Tokyo, Japan) supplemented with 0.1% bovine serum albumin (BSA; Wako Pure Chemical Industries, Ltd., Osaka, Japan) and washed three times by centrifugation at 1000×*g* for 4 min. After washing, the precipitated sperm pellet was resuspended in porcine fertilization medium (PFM; Research Institute for Functional Peptides, Yamagata, Japan) at a concentration of 1×10^7 cells/ml [25]. For insemination, 20 cumulus–oocyte complexes that had been matured in vitro were placed in a 100-μl drop of PFM containing spermatozoa (5.0×10^4 cells/ml); the oocytes and sperm were incubated for 8 h

at 38.5 °C in a humidified atmosphere containing 5% CO_2, 5% O_2, and 90% N_2. After insemination, the eggs were transferred to HEPES–TL–polyvinylpyrrolidone (PVP) membranes and cumulus cells and excess sperm were removed by gentle pipetting. Putative zygotes showing the release of two polar bodies with normal cytoplasmic morphology were selected for cytoplasmic injection. All parthenogenetic embryos produced were used for cytoplasmic injection, provided that they had a normal cytoplasmic morphology. Both parthenogenetic and in vitro-fertilized embryos were confirmed by preliminary experiments to be in the pronuclear stage.

2.5. Cytoplasmic injection

Cytoplasmic injection of the genome-editing molecules was performed 4.5–6 h after electrical activation of the parthenotes or 9–10 h after insemination of IVM/IVF-derived zygotes. Microinjection was performed using an inverted microscope equipped with a micromanipulator (MD-102; Narishige, Tokyo, Japan) and an air injector (IG-2, S. Co., Ltd., Tokyo, Japan). For analyzing the blastocysts for genome editing efficiency, the injected embryos were cultured in porcine zygote medium (PZM)-5 for 4 d and then cultured until day 7 in PZM-5 supplemented with 10% fetal bovine serum (FBS). After 7 d of culture, blastocysts that developed from the injected embryos were harvested for mutation analysis. For the generation of fetuses, injected embryos were transferred at the 1- to 8-cell stage to recipient gilts after culturing for 1 or 2 d.

2.6. Embryo transfer

Crossbred (Large White/Landrace × Duroc) prepubertal gilts weighing 100–105 kg were used as recipients of the injected embryos. The gilts were each administered a single intramuscular injection of 1000 IU of equine chorionic gonadotropin (eCG; ASKA Pharmaceutical, Tokyo, Japan) to induce estrus. Ovulation was induced by an intramuscular injection of 1500 IU of human chorionic gonadotropin (hCG; Kyoritsu Seiyaku, Tokyo, Japan) 66 h after the eCG injection. Injected embryos cultured for 1–2 d were surgically transferred into the oviducts of recipient gilts 49–50 h after hCG injection under general anesthesia.

2.7. Analysis of CRISPR-Cas9-induced mutations

The target region of porcine *IGF1R*-targeted CRISPR-Cas9 was amplified from blastocysts by direct PCR using MightyAmp DNA Polymerase Ver. 2 (Takara Bio, Shiga, Japan) and the corresponding primers (Supplementary Table 1). For the analysis of mutations in fetuses, genomic DNA was extracted from the tail of the fetuses using a DNeasy Blood and Tissue Kit (Qiagen, Hilden, Germany), and the target region was amplified using PrimeSTAR GXL DNA polymerase (Takara Bio). Subsequently, the PCR fragments were examined using the BigDye Terminator Cycle Sequencing Kit, an Applied Biosystems 3500xl Genetic Analyzer (Thermo Fisher Scientific), and appropriate primers (Supplementary Table 1). The PCR products were cloned and sequenced using the Zero Blunt TOPO PCR Cloning Kit (Thermo Fisher Scientific). For some fetuses, further analysis to detect large deletions was performed using appropriate primers (Supplementary Table 2). The mutation sequences were determined using Sanger sequencing, as described above.

2.8. IGF1R-gene-knockout porcine fetuses

Previous studies had shown that *Igf1r*-KO mice die soon after birth due to respiratory failure caused by insufficient muscle strength, especially of the respiratory muscles (20, 26). Therefore, in the current study, the fetuses were removed by cesarean section at 104 d of fetal age and evaluated thereafter. WT fetuses at day 104 were used for validation.

2.9. Western blot analysis

Organ tissues at the same age from *IGF1R*–KO and WT pigs were homogenized in RIPA buffer (Thermo Fisher Scientific, Waltham, MA, USA) with a protease inhibitor cocktail (Nacalai Tesque Inc., Kyoto, Japan), then centrifuged, and the supernatants were collected. Protein concentrations of the samples were quantified using a detergent-compatible protein assay (Bio-Rad, Hercules, CA, USA) based on the Lowry method. The protein lysates mixed with equal volume of 2 × Sample Buffer Solution with 2-mercaptoethanol (Nacalai Tesque Inc.) were boiled at 95 °C for 5 min. Proteins were resolved using Any kD Mini-PROTEAN TGX precast polyacrylamide gel (Bio-Rad) and transferred to a PVDF membrane (Cytiva, Marlborough, MA, USA) using a Mini Trans-Blot Electric Transfer Cell (Bio-Rad) at 25 V for 30 min. The membranes were blocked for 30 min at room temperature using Blocking One (Nacalai Tesque, Inc.). After blocking, the membranes were incubated with an anti-IGF1R antibody (1:200 dilution; Santa Cruz Biotechnology, Dallas, TX, USA) and with anti-β-actin antibody (1:5000 dilution; ABM, Richmond, BC, Canada), respectively, for 1 h at room temperature and subsequently incubated with HRP-conjugated anti-mouse IgG antibody (1:5000 dilution; Santa Cruz Biotechnology) for 1 h at room temperature. After washing three times with PBS, signals were detected using ECL Prime Western Blotting Detection Reagent (Cytiva) in the iBright FL1500 Imaging System (Thermo Fisher Scientific).

2.10. Immunohistochemical analysis

Tissue samples were fixed in a 4% paraformaldehyde solution (FUJIFILM Wako Pure Chemical Corporation, Osaka, Japan), embedded in paraffin, sectioned, and stained with hematoxylin & eosin using standard methods. For immunohistochemical analysis, the fixed sections were treated with IGF1Rβ/IGF1R Antibody (Santa Cruz Biotechnology; 1:50 dilution) overnight at 4 °C. After removing the excess antibody, the sections were incubated with Histofine Simple Stain MAX PO (MULTI) (Nichirei Bioscience) and DAB chromogen for 30 min at 25 °C. Slides were counterstained with hematoxylin and visualized under a BIOREVO BZ9000 microscope (Keyence, Osaka, Japan).

2.11. Statistical analysis

Statistical analyses were performed using SPSS software v26 (IBM SPSS, Chicago, IL, USA). Data are presented as the mean ± standard error of the mean (SEM). Welch's *t*-test was used to evaluate the differences in numerical data between *IGF1R*- KO and WT porcine fetuses. Differences were considered statistically significant at $P < 0.05$.

3. Results

3.1. Selection of designed gRNAs for IGF1R–KO generation

To generate IGF1R–KO pigs, we attempted to induce mutations in the IGF1R gene using CRISPR/Cas9 targeting exons 2 and 9 in the IGF1R gene locus (Fig. 1). Three gRNAs were prepared for each of exons 2 and 9. To evaluate the genome-targeting efficiency of various gRNA concentrations, a nuclease-based mutation detection assay was performed. Genomic DNA was extracted from fibroblasts for IGF1R locus analysis by tracking indels via decomposition.

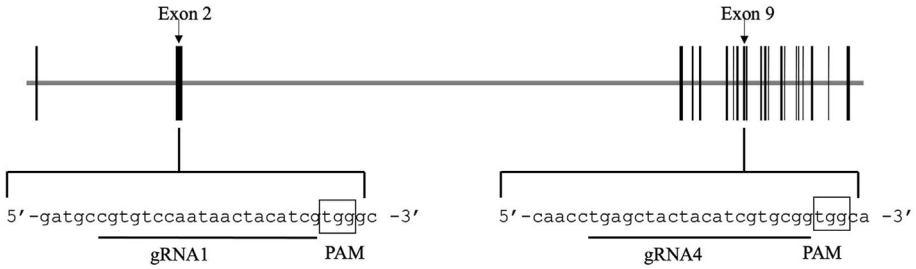

Fig. 1. Generation of *IGF1R*-gene-knockout porcine fetuses by genome editing. Schematic structure of the porcine IGF1R gene, which consists of 21 exons, and the design of CRISPR-Cas9 targeting the IGF1R gene. The coding regions are indicated by black vertical lines. Two different gRNAs (gRNA1 and gRNA4) designed in exons 2 and 9 and used for the generation of *IGF1R*-gene-knockout fetuses are shown. The gRNAs and protospacer adjacent motif (PAM) sequences are underlined and boxed, respectively.

Subsequently, the efficiency of mutation induction by the cytoplasmic injection of *IGF1R*-targeted CRISPR-Cas9 into parthenogenetic embryos was evaluated. Blastocyst formation and mutation rates were compared for various concentrations of guide RNA (gRNA; 5–20 ng/μl) and Cas9 (20–50 ng/μl). Comparing the three different concentrations of each guide RNA in exon 2, the indels of gRNA1 and gRNA3 showed similar results (Fig. 2A); gRNA1 induced 100% mutation and 80% of biallelic mutation rates (Table 1). The same evaluation was performed using exon 9 (Fig. 2A). Upon cytoplasmic injection into porcine parthenogenetic embryos at the pronuclear stage, none of the tested gRNAs was found to be associated with blastocyst morphology (Fig. 2B); gRNA1 and gRNA 4 were used in subsequent experiments.

3.2. Generation of IGF1R–KO porcine fetuses

CRISPR-Cas9 molecules were injected into the cytoplasm of in vitro-fertilized embryos at the pronuclear stage. Morphology of

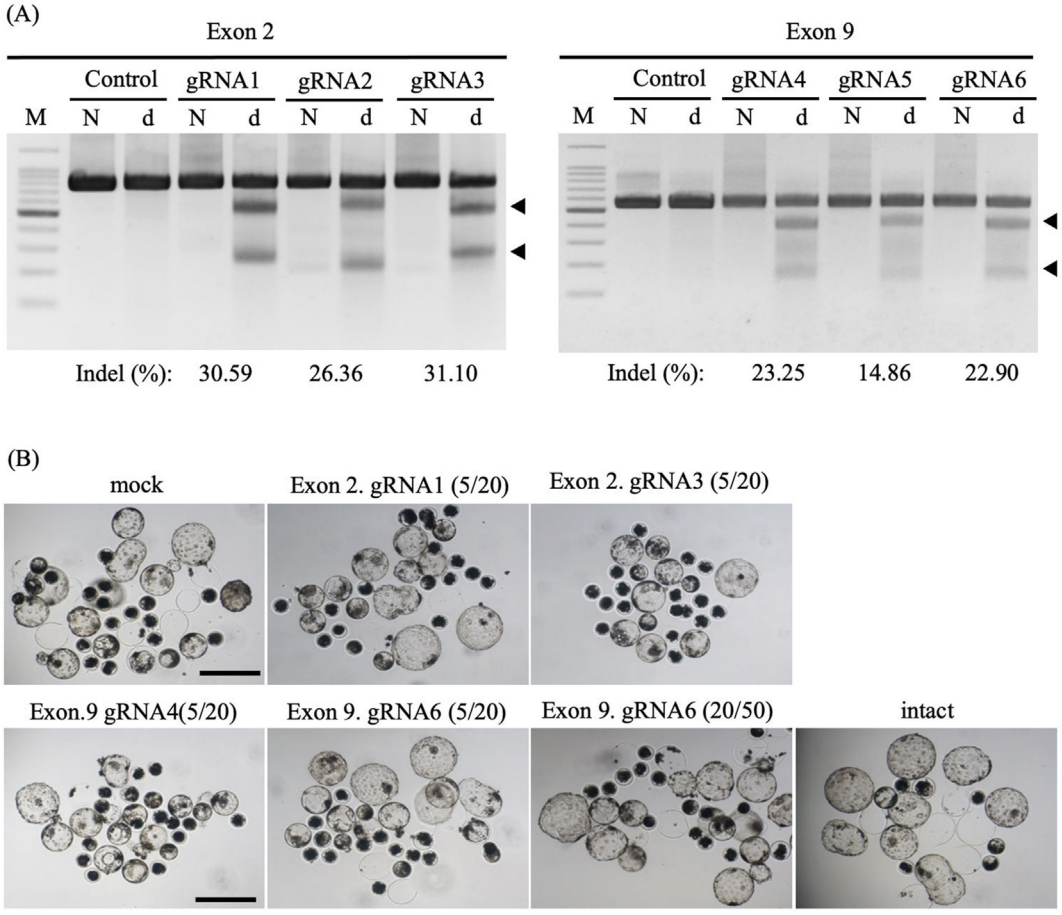

Fig. 2. Evaluation of each *IGF1R*-targeting guide RNA. (A) Guide RNA (gRNA) of various concentrations was used in nuclease based-mutation detection assays to determine the genome targeting efficiency. Genomic DNA was extracted from fibroblasts for *IGF1R*-locus analysis tracking indels by decomposition. Subsequently, the efficiency of mutation induction by cytoplasmic injection of *IGF1R*-targeted CRISPR-Cas9 into parthenogenetic embryos was evaluated. N: non-digest, d: nuclease-digest, Indel: insertion/deletion. (B) Blastocyst formation was compared for various concentrations of each guide RNA (Exon 2: gRNA; 5 ng/μl and Exon 9: gRNA; 2–20 ng/μl). Blastocyst formation rates for each of exons 2 and 9 were reliable (exon 2: 41.7–42.1%, exon 9: 50.7–64.4%). Scale: 500 μm.

Table 1
Incidence of mutations in porcine embryos after cytoplasmic injection of CRISPR -Cas9 protein targeting the *IGF1R* gene.

Target region and type of gRNA	gRNA (ng/μl)	Cas9 protein (ng/μl)	Embryos cultured	Embryos cleaved (%)	Embryos developed to blastocysts (%)	Blastocysts analyzed	Blastocysts with:		
							mutations (%)	Monoallelic mutations (%)	Biallelic mutations (%)
mock	0	0	85	68 (80.0)	45 (52.9)	NA	NA	NA	NA
Exon 2. gRNA1	5	20	60	52 (86.7)	25 (41.7)	15	15 (100)	3 (21.4)	12 (80.0)
Exon 2. gRNA3	5	20	57	49 (86.0)	24 (42.1)	16	12 (75.0)	7 (58.3)	5 (41.6)
Exon 9. gRNA4	5	20	71	55 (77.5)	36 (50.7)	14	14 (100)	0 (0)	14 (100)
Exon 9. gRNA5	20	50	68	48 (70.6)	40 (58.8)	14	14 (100)	0 (0)	14 (100)
Exon 9. gRNA6	5	20	59	53 (89.8)	38 (64.4)	16	12 (75.0)	11 (91.6)	1 (8.3)
intact	–	–	45	37 (82.2)	29 (64.4)	NA	NA	NA	NA

the injected embryos before transfer was normal, indicating that embryonic development was unaffected (Supplementary Fig. 1). Embryos injected with two different gRNAs were transplanted independently into different recipients, yielding 15 offspring in total (Tables 2 and 3). Genetic analysis detected mutant IGF1R sequences in six offspring, five of which were biallelic (Table 2). Injection of gRNA1 produced nine fetuses and a monoallelic mutation was confirmed in one fetus (Table 3). Injection of gRNA4 led to six fetuses without any monoallelic mutation (Table 2). One of gRNA1 and four from gRNA4 injections yielded IGF1R–KO fetuses (Table 3). Genomic DNA analysis revealed homozygous frameshift mutations or large deletions in IGF1R–KO fetuses. Injection of two different gRNAs resulted in the same phenotype in IGF1R–KO fetuses. Thus, these phenotypes appeared for reasons other than off-target mutations.

3.3. Overall appearance of IGF1R-gene-knockout porcine fetuses

IGF1R–KO fetuses at 104 days of fetal age were smaller than WT fetuses at 104 d (Figs. 3 and 4). They had severely blunted somatic growth. Their thymus and lungs were smaller than those of the WT fetuses. The characteristic findings included the impact of IGF1R–KO on skin development. The epidermis was underdeveloped and characterized by a very thin spinous layer. A monoallelic mutation in the fetuses resulted in the same body size as the WT (data not shown).

3.4. Phenotype of porcine IGF1R-gene-knockout fetuses

Organ to body weight ratios of *IGF1R*–KO and WT fetuses at 104 days of fetal age were compared. Most organs of endodermal origin, including the liver and pancreas, showed a remarkable increase in size of *IGF1R*–KO fetuses (Fig. 4B). The kidneys of mesodermal origin, when compared between KO and WT pigs, were larger in KO pigs. Although the thymus is of endodermal origin, it was significantly smaller than in WT fetuses. No difference was observed between *IGF1R*–KO male and female fetuses.

Table 3
Generation of *IGF1R* -knockout pigs using 2 different genomes editing with CRISPR -Cas9.

Target region and type of gRNA	Fetuses No.	sex	genotype
Exson2 (gRNA1)	K363-1	female	WT
	K363-2	male	WT
	K363-3	male	WT
	K363-4	female	WT
	K363-5	male	WT
	K363-6	female	WT
	K363-7	female	1bp ins/23bp del
	K363-8	female	WT
	K363-9	male	1bp ins/WT (hetero)
Exson 9 (gRNA4)	K366-1	male	WT
	K366-2	male	4bp del/4bp del
	K366-3	female	5bp del/4266bp del
	K366-4	male	4bp del/5bp del
	K366-5	female	2518bp del/2518bp del
	K366-6	male	WT

3.5. Histological analyses and comparison

Histopathological examination revealed no particular organ abnormality among those explored in this study. *Igf1r*-KO mice usually die of respiratory failure due to underdeveloped muscles [21,26]; however, no abnormality was found in the lung tissue of the *IGF1R*–KO fetuses. No structural block was confirmed in the bronchi or upper respiratory tract and the alveolar epithelium of *IGF1R*–KO fetuses was indistinguishable from that of WT fetuses. The thymus was smaller in *IGF1R*–KO fetuses, although the cells were of the same size as in the WT ones. The liver and pancreas were clearly larger in the KO fetuses than in the WT fetuses; however, no abnormality was seen in the cells. IGF1R protein was detected in the organs of the WT but not in those of *IGF1R*–KO fetuses (Fig. 5B and C).

4. Discussion

In this study, a genome-editing approach was used to generate *IGF1R*–KO pigs by injecting genome-editing molecules into the

Table 2
Generation of *IGF1R* -knockout pigs by cytoplasmic injection of CRISPR-Cas9 into porcine zygotes.

Target region and type of gRNA(concentration: gRNA/Cas9)	Recipient No.	Embryos injected[a]	Embryos transferred	Embryonic stage at transfer	Pregnancy	Fetuses obtained[b]	Fetuses with:		
							Mutations (%)	Monoallelic mutations (%)	Biallelic mutations (%)
Exon 2 gRNA1 (5/20 ng/μl)	K363	163	71	2- 8 cell	+	9	2 (22.2)	1 (11.1)	1 (11.1)
Exon 9 gRNA4 (5/20 ng/μl)	K366	191	102	1- 2 cell	+	6	4 (66.7)	0 (0)	4 (66.7)

[a] IVM/IVF -derived embryos at the pronuclear stage.
[b] Fetuses were obtained at day 104 of gestation.

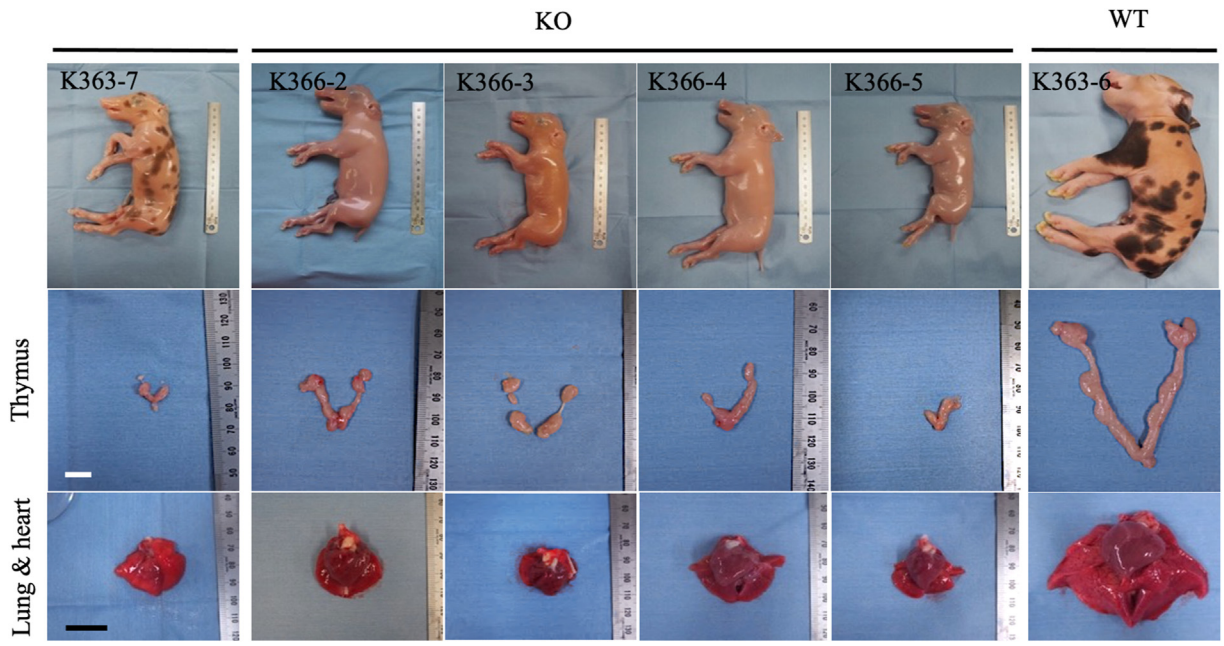

Fig. 3. Appearance of *IGF1R*–KO porcine fetuses. *IGF1R*–KO fetuses were obtained by anatomical dissection at 104 d of fetal age. The phenotype differs from that of *IGF1R*–KO fetuses not only in the size of the bodies, thymus, and lungs, but also in the appearance of the skin, which is markedly opaque. The translucent skin of the *IGF1R*–KO fetuses was notable. K363-7 (KO female. exon 2: gRNA1) and K363-6 (WT female) were obtained from the same litter. K366: 2–5 (KO. exon 9: gRNA4). KO: knockout, WT: wild type. Scale bars: white = 1 cm; black = 2 cm.

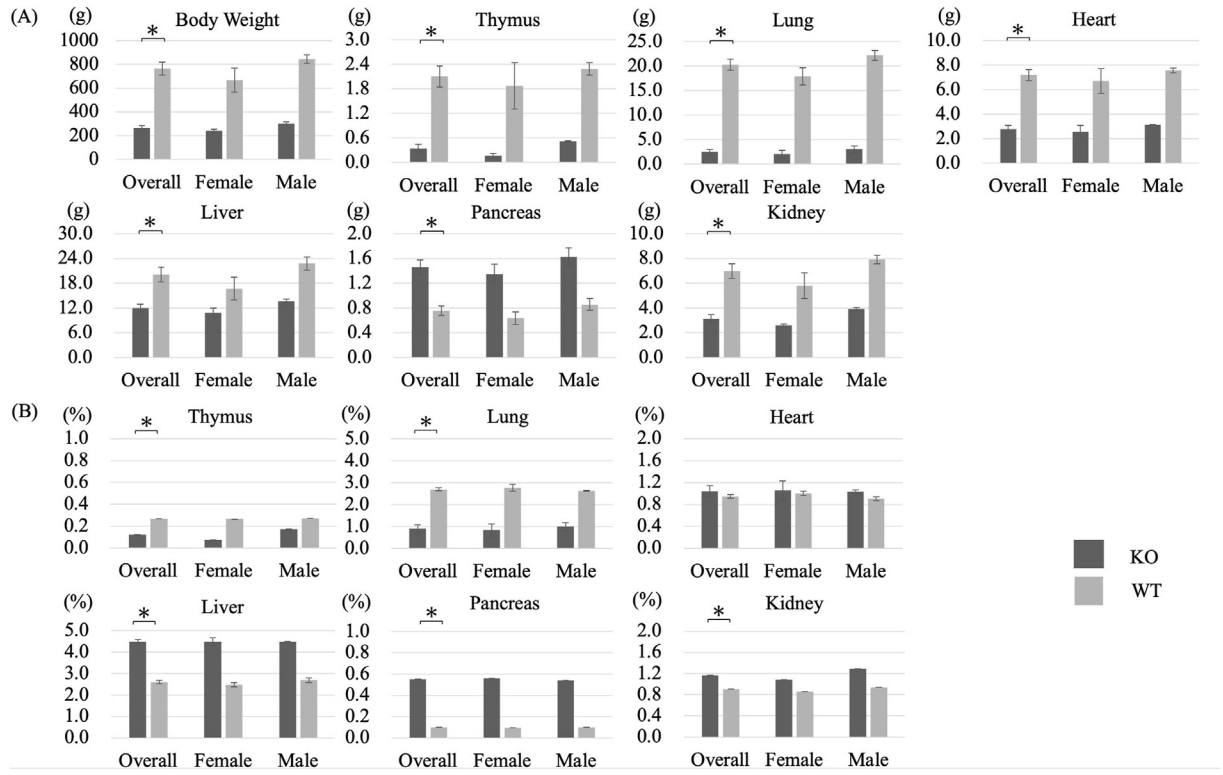

Fig. 4. Body and organ weight ratios of *IGF1R*–KO porcine fetuses. Wet organ weight was determined by anatomic dissection at 104 d of fetal age. (A) Body weight and organ weight. The three graphs compare KO and WT, and male and female KO porcine fetuses. (B) Each organ is represented as organ per unit body weight. Quantitative data are presented as means ± standard error of mean. KO: knockout, WT: wild type. *IGF1R*–KO fetuses: n = 5 (3 females and 2 males), WT fetuses: n = 9; *P < 0.05 versus WT.

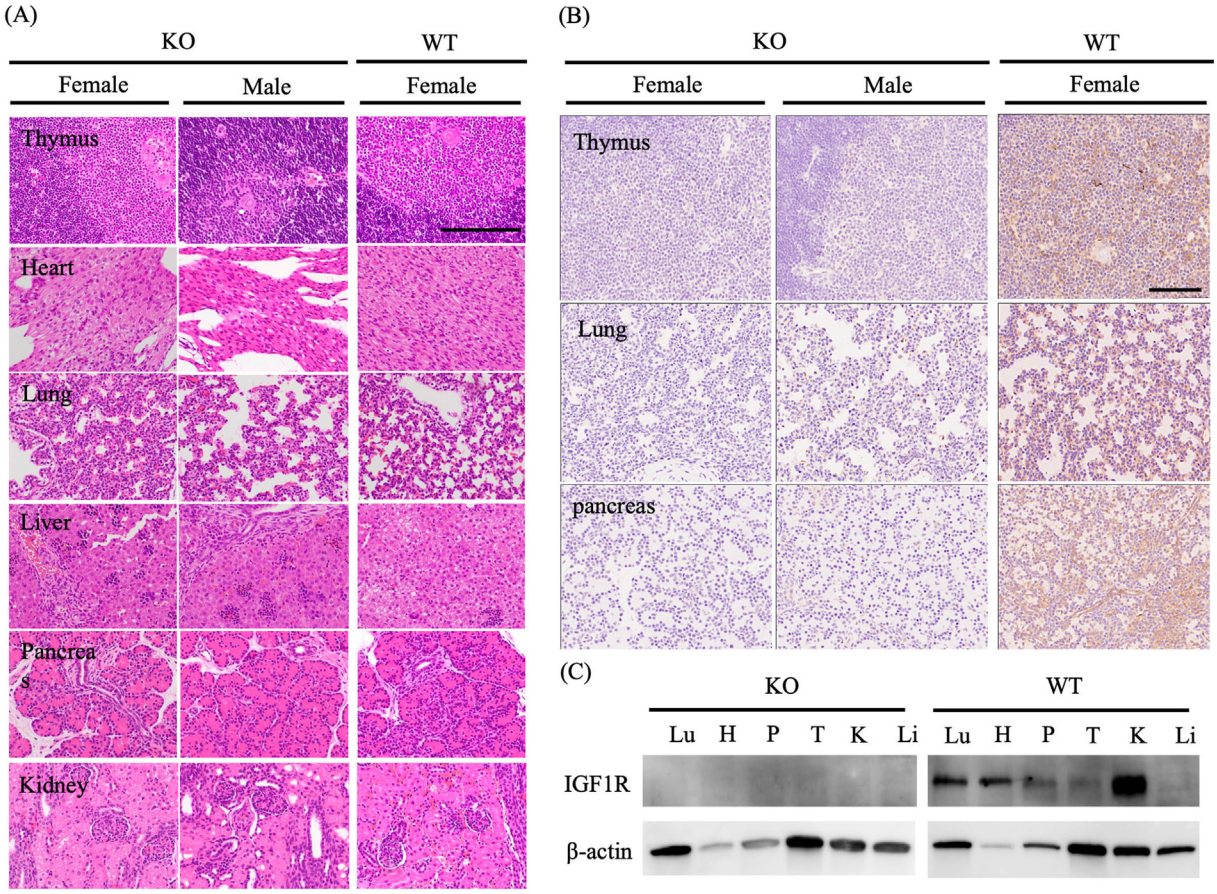

Fig. 5. Histological appearance of organs of *IGF1R*–KO porcine fetuses obtained by anatomical dissection at 104 d of fetal age. (A–C) Hematoxylin and eosin (H&E) staining (A), IGF1R staining (B), and Western blot analysis (C) are shown. (A) H&E staining of each organ of *IGF1R*–KO porcine fetuses at 104 d of age. There was no apparent difference between KO and WT fetuses in any organ. (B) Immunohistochemical staining of IGF1 in each organ of *IGF1R*–KO porcine fetuses at 104 d of age. IGF1R staining was negative in each organ of the KO fetuses and positive in the WT fetuses. KO involved a K366-3 female and a K366-2 male. WT was a K366-6 female. KO: knockout, WT: wild type. Scale bar: 100 μm. (C) Western blotting was negative for all organs tested in KO fetuses. Lu: lungs, H: heart, P: pancreas, T: thymus, K: kidneys, Li: liver. KO: knockout, WT: wild type.

cytoplasm of porcine zygotes. *Igf1r*-KO has already been achieved in mice [20,21,27] and has been used to achieve *in vivo* organogenesis via a strategy to open a cell-competitive niche. *Nishimura* et al. reported how rat donor cells gradually replaced mouse host cells in the organs of *Igf1r*-KO mice [18]; *Igf1r* is a gene expressed not only in rodents but is widely conserved among mammals, including humans [27]. Therefore, if the phenotype of *Igf1r*-KO mice could be reproduced in large animals, such as pigs, it would advance the generation of human organs in the interspecies organ niche.

To generate *IGF1R*–KO pigs, two different gRNAs were designed and cytoplasmic injection into the zygote was done. This method has been successfully used in pigs to generate KO animals [24,28,29] but has the disadvantage of generating mosaic individuals with mutations [24,30,31]. Currently, there is no reliable method to prevent the development of mosaicism. In the present study, mosaicism was observed in one of the 15 animals generated (Ex. 2 (gRNA1) K363-9). The generated pigs did not differ from WT pigs in terms of appearance, size, and organ size (data not shown). Rather, when two gRNAs were used to generate KO pigs in two independent trials, the generated KO pigs showed similar phenotypes, indicating that this was not an off-target phenotype.

Previous studies in mice had shown that *Igf1r*-KO animals invariably die soon after birth due to respiratory and severe growth failure. The mice are born alive but develop cyanosis despite respiratory efforts and die within minutes [20,26]. Therefore, the fetuses were retrieved by cesarean section at 104 d of fetal age for validation purposes.

The comparison of *IGF1R*–KO and 104-day-old WT fetuses evidenced growth defects and very thin skin in *IGF1R*–KO fetuses. This was also reported in mice shortly before birth. The epidermis of these mice was found to have fewer echinocyte layers and hair follicles than that of WT mice [21,32]. The endoderm-derived organs, liver and pancreas, were significantly enlarged in *Igf1r*-KO mice [33]. In the *IGF1R*–KO fetuses in this validation, both organs were larger than those in the WT fetuses. The reason for the larger pancreas in *Igf1r*-KO animals is clear from the mouse validation; the enlargement was due to the upregulation of growth hormone (GH) [34]. Oversecretion of GH leads to high blood glucose levels and compensatory enlargement of the pancreas to control blood glucose and glucose intolerance [33]. In *IGF1R*–KO pigs, measurement of the GH and insulin levels would be essential; however, blood samples from 104-day-old fetuses are extremely difficult to obtain.

The liver and kidneys of *IGF1R*–KO fetuses were also larger than the WT organs based on body weight. In the *IGF1R*–KO pigs generated in this study, almost all organs tested had the same

phenotype as in mice; the only organ that differed was the thymus, which was reported to be larger in *Igf1r*-KO mice than in WT mice [33]. In all species, the higher the expression of *Igf1r*, the smaller the organ in *Igf1r*-KO animals; reads per kilobase million (RPKM) of *Igf1r* may provide clues as to why the thymus is inconsistent with this tendency. For example, in the liver, RPKM was 1.121 ± 0.19 in pigs [35] and 0.988 at 18 d of fetal age and 0.158 in adult mice [36]. The RPKM in the heart was 1.95 ± 0.458 in pigs and 1.944 in mice. KO-pig organs were larger than WT organs. Pigs and mice showed similar tendencies in the liver and heart. In the lungs, the RPKM is 0.813 ± 0.35 in pigs [35] and 5.941 in adult mice [36]. However, in the lungs, both animals showed differences despite being hypomorphic; therefore, RPKM of *Igf1r* alone does not explain this difference. Reports of RPKM in KO pigs and mice are limited to some organs only, excluding the muscle, pancreas, or thymus; therefore, comparing them any further was impossible. For this reason, the study was also validated using embryology. The thymus, thyroid, trachea, lungs, and esophagus originate from the endoderm, most notably from the anterior foregut [37]. In addition, lymphocytes occupying the thymus are derived from the mesoderm (the lateral plate mesoderm [38]), and organs of mesodermal origin in *Igf1r*-KO animals show hypoplasia [32,33] (Fig. 5A). Since the thymus is of the same origin as the hypoplastic lungs, and lymphocytes occupying the thymus are of mesodermal origin, a combination of these circumstances led to the smaller thymus in the *IGF1R*−KO fetuses.

Histopathological examination of *Igf1r*-KO mice showed no lung abnormality [20], and the cause of respiratory failure was the extremely fragile development of intercostal muscles [20,26,39]. In the validation by *Epaud* et al., the muscle group of the same litter of WT and KO mice at E16.5−E18.5 was examined and a number of muscle cells were found to be affected [26]. Although the lungs were smaller in the *IGF1R*−KO fetuses, histological examination of the lungs did not reveal any abnormalities in organ architecture. The reduced body weight of these pig fetuses could be a consequence of a decrease in tissue cell number (hypoplasia) and not in cell size, based on comparisons of cell dimensions in the thymus, lungs, liver, and pancreas with those of age-matched WTs. The difference in organ size reflected the difference in the number of cells that constituted the organ.

An important question is how the *Igf1r* gene KO in humans compares with that in mice or pigs. There are no reports of KO of the *Igf1r* gene in humans. However, there are some reports of mutations of the *Igf1r* gene [40−43]. In human cases, isolated mutation of the *Igf1r* gene do not occur; the *Igf1r* gene is located on chromosome 15 and is therefore affected by deletion of chromosome 15. The *Igf1r* gene is known to play an essential role in human intrauterine and postnatal development [42]. Indeed, several heterozygous *Igf1r* gene mutations have recently been identified in humans with intrauterine or postnatal growth retardation [40−42]. As mutation of the *Igf1r* gene has been repeatedly reported to be associated with intrauterine growth retardation, *Nagai* et al. speculated that the dosage of the *Igf1r* gene may have determined the growth in these children. Heterozygous mutations in human IGF1R are associated with delayed growth and sometimes delayed mental development; lung hypoplasia has been reported in a patient with a deletion in the distal long arm of chromosome 15 containing the *Igf1r* gene, but rarely with altered respiratory function [43]. Why do people with a mutated *Igf1r* gene survive? Validation in mice showed that a wild-type IGF1R protein level of approximately 22% was sufficient for the minimum lung function required for survival [26]. A human may not be able to live with a complete KO of the *Igf1r* gene, but with some expression of the *Igf1r* gene, it may be possible to survive although the lungs may be hypoplastic.

The *IGF1R*−KO pigs generated in this study closely reproduced the mouse and human phenotypes and were highly reproducible. Interspecies organogenesis using blastocyst complementation has been successful in rodents, but not in evolutionarily-distant species. In distant species, generating blastocysts using cells from the two species is extremely difficult (unpublished data), and even when blastocysts are generated, the formation of highly chimeric fetuses is prevented. In *Igf1r*-KO mice, the permissive niche did not affect early embryonic development; donor chimerism gradually increased from embryonic day 11 and sometimes dominated the entire organ [18]. In other words, deletion of *Igf1r* avoided early developmental arrest of recipient cells such that interspecific fetuses with high levels of organ chimerism could be produced by blastocyst complementation with developmentally-compatible, xenogenic pluripotent stem cells. In order for human PSCs to be cooperatively integrated into the embryogenesis process from the blastocyst to the gastrulation stage in pigs, molecular compatibility, including cell adhesion and differentiation molecules, are crucial. Furthermore, synchrony in cell proliferation between the two species is a key factor in establishing coordinated interspecies chimerism, from the pre-implantation stage to fetal development. The fulfillment of these conditions with the cell-competitive niche created by *Igf1r* gene KO should facilitate the formation of interspecies chimerism between pigs and evolutionarily-distant species, including humans. Blastocyst complementation experiments with pigs and monkeys will allow us to validate the efficacy of the *Igf1r* gene KO trait for the formation of interspecific chimeras.

5. Conclusions

The *IGF1R*−KO pigs generated in this study almost reproduced the mouse phenotype and were highly reproducible. The current generation of *IGF1R*−KO pigs is expected to facilitate the contribution of donor cells to host tissues, thereby enabling the generation of organs through blastocyst complementation with developmentally-compatible, xenogeneic pluripotent stem cells over a wide evolutionary distance.

Funding

This research work was supported by Grants-in-Aid for Scientific Research of Japan (24K02513 to M. Nag), the Japan Agency for Medical Research and Development (Leading Advanced Projects for Medical Innovation [LEAP]), Generation of Functional Organs using Developmental Niche (to H. Nak), Japan Science and Technology Agency (Exploratory Research for Advanced Technology [ERATO]), NAKAUCHI Stem Cell and Organ Regeneration (to H. Nak.), CIRM (LA1_C12-06917; DISC1-10555) and the Ludwig Foundation (to H. Nak.), and the Meiji University International Institute for Bio-Resource Research (to H. Nag). The funding organizations had no roles in the study's design, data collection and analysis, the decision to publish, or the manuscript's preparation.

List each author's specific contributions to the work

M.Nag., T.N., H.Nak, and H. Nag. conception and design, financial support, collection and assembly of data, data analysis and interpretation, manuscript writing, and final approval of manuscript.

A.Y, K.N, M.W, H.M, N.Miz and K.U collection and assembly of data, data analysis and interpretation.

Declaration of competing interest

H.Nagashima is a founder and shareholder of PorMedTec Co., Ltd. These associations do not alter the authors' adherence to the journal's policies on sharing data and materials. The other authors declare that they have no conflicts of interest.

Acknowledgments

We thank Dr. Erica Furukawa for technical assistance. This research work was supported by Grants-in-Aid for Scientific Research of Japan (24K02513 to M. Nag), the Japan Agency for Medical Research and Development (Leading Advanced Projects for Medical Innovation [LEAP]), Generation of Functional Organs using Developmental Niche (to H. Nak), Japan Science and Technology Agency (Exploratory Research for Advanced Technology [ERATO]), NAKAUCHI Stem Cell and Organ Regeneration (to H. Nak.), CIRM (LA1_C12-06917; DISC1-10555) and the Ludwig Foundation (to H. Nak.), and the Meiji University International Institute for Bio-Resource Research (to H. Nag). The funding organizations had no roles in the study's design, data collection and analysis, the decision to publish, or the manuscript's preparation.

Appendix A. Supplementary data

Supplementary data to this article can be found online at https://doi.org/10.1016/j.reth.2024.08.025.

References

[1] De Luca M, Aiuti A, Cossu G, Parmar M, Pellegrini G, Robey PG. Advances in stem cell research and therapeutic development. Nat Cell Biol 2019;21:801. 1.
[2] Takebe T, Wells JM. Organoids by design. Science 2019;364:956–9.
[3] Goto T, Hara H, Sanbo M, Masaki H, Sato H, Yamaguchi T, et al. Generation of pluripotent stem cell-derived mouse kidneys in Sall1-targeted anephric rats. Nat Commun 2019;10:451.
[4] Isotani A, Hatayama H, Kaseda K, Ikawa M, Okabe M. Formation of a thymus from rat ES cells in xenogeneic nude mouse↔rat ES chimeras. Gene Cell 2011;16:397–405.
[5] Kobayashi T, Yamaguchi T, Hamanaka S, Kato-Itoh M, Yamazaki Y, Ibata M, et al. Generation of rat pancreas in mouse by interspecific blastocyst injection of pluripotent stem cells. Cell 2010;142:787–99.
[6] Yamaguchi T, Sato H, Kato-Itoh M, Goto T, Hara H, Sanbo M, et al. Interspecies organogenesis generates autologous functional islets. Nature 2017;542:191–6.
[7] Shalaby F, Rossant J, Yamaguchi TP, Gertsenstein M, Wu XF, Breitman ML, et al. Failure of blood-island formation and vasculogenesis in Flk-1-deficient mice. Nature 1995;376:62–6.
[8] Romano R, Palamaro L, Fusco A, Giardino G, Gallo V, Del Vecchio L, et al. FOXN1: a master regulator gene of thymic epithelial development program. Front Immunol 2013;4:187.
[9] Marcos S, González-Lázaro M, Beccari L, Carramolino L, Martin-Bermejo MJ, Amarie O, et al. Meis1 coordinates a network of genes implicated in eye development and microphthalmia. Development 2015;142:3009–20.
[10] Caprioli A, Villasenor A, Wylie LA, Braitsch C, Marty-Santos L, Barry D, et al. Wnt4 is essential to normal mammalian lung development. Dev Biol 2015;406:222–34.
[11] Offield MF, Jetton TL, Labosky PA, Ray M, Stein RW, Magnuson MA, et al. PDX-1 is required for pancreatic outgrowth and differentiation of the rostral duodenum. Development 1996;122:983–95.
[12] Nishinakamura R, Matsumoto Y, Nakao K, Nakamura K, Sato A, Copeland NG, et al. Murine homolog of SALL1 is essential for ureteric bud invasion in kidney development. Development 2001;128:3105–15.
[13] Goto T, Hara H, Nakauchi H, Hochi S, Hirabayashi M. Hypomorphic phenotype of Foxn1 gene-modified rats by CRISPR/Cas9 system. Transgenic Res 2016;25:533–44.
[14] Usui J, Kobayashi T, Yamaguchi T, Knisely AS, Nishinakamura R, Nakauchi H. Generation of kidney from pluripotent stem cells via blastocyst complementation. Am J Pathol 2012;180:2417–26.
[15] Matsunari H, Watanabe M, Hasegawa K, Uchikura A, Nakano K, Umeyama K, et al. Compensation of disabled organogeneses in genetically modified pig fetuseses by blastocyst complementation. Stem Cell Rep 2020;14:21–33.
[16] Wu J, Platero-Luengo A, Sakurai M, Sugawara A, Gil MA, Yamauchi T, et al. Interspecies chimerism with mammalian pluripotent stem cells. Cell 2017;168:473–486.e15.
[17] Yamaguchi T, Sato H, Kobayashi T, Kato-Itoh M, Goto T, Hara H, et al. An interspecies barrier to tetraploid complementation and chimera formation. Sci Rep 2018;8:15289.
[18] Nishimura T, Suchy FP, Bhadury J, Igarashi KJ, Charlesworth CT, Nakauchi H. Generation of functional organs using a cell-competitive niche in intra- and inter-species rodent chimeras. Cell Stem Cell 2021;28:141–9.
[19] Yamanaka S, Saito Y, Fujimoto T, Takamura T, Tajiri S, Matsumoto K, et al. Kidney regeneration in later-stage mouse embryos *via* transplanted renal progenitor cells. J Am Soc Nephrol 2019;30:2293–305.
[20] Baker J, Liu JP, Robertson EJ, Efstratiadis A. Role of insulin-like growth factors in embryonic and postnatal growth. Cell 1993;75:73–82.
[21] Liu JP, Baker J, Perkins AS, Robertson EJ, Efstratiadis A. Mice carrying null mutations of the genes encoding insulin-like growth factor I (Igf-1) and type 1 IGF receptor (IGF1R -). Cell 1993;75:59–72.
[22] Lupu F, Terwilliger JD, Lee K, Segre GV, Efstratiadis A. Roles of growth hormone and insulin-like growth factor 1 in mouse postnatal growth. Dev Biol 2001;229:141–62.
[23] Bentov I, Werner H. Insulin-like growth factor-1. In: Kastin AJ, editor. Handbook of biologically active Peptides. second ed. Academic Press; 2013. p. 1627–32.
[24] Watanabe M, Nakano K, Uchikura A, Matsunari H, Yashima S, Umeyama K, et al. Anephrogenic phenotype induced by SALL1 gene knockout in pigs. Sci Rep 2019;9:8016.
[25] Yoshioka K. Development and application of a chemically defined medium for the in vitro production of porcine embryos. J Reprod Dev 2011;57:9–16.
[26] Epaud R, Aubey F, Xu J, Chaker Z, Clemessy M, Dautin A, et al. Knockout of insulin-like growth factor-1 receptor impairs distal lung morphogenesis. PLoS One 2012;7:e48071.
[27] Rotwein P. Diversification of the insulin-like growth factor 1 gene in mammals. PLoS One 2017;12:e0189642.
[28] Wang H, Yang H, Shivalila CS, Dawlaty MM, Cheng AW, Zhang F, et al. One-step generation of mice carrying mutations in multiple genes by CRISPR/Cas-mediated genome engineering. Cell 2013;153:910–8.
[29] Shen B, Zhang J, Wu H, Wang J, Ma K, Li Z, et al. Generation of gene-modified mice via Cas9/RNA-mediated gene targeting. Cell Res 2013;23:720–3.
[30] Li D, Qiu Z, Shao Y, Chen Y, Guan Y, Liu M, et al. Heritable gene targeting in the mouse and rat using a CRISPR-Cas system. Nat Biotechnol 2013;31:681–3.
[31] Sung YH, Kim JM, Kim HT, Lee J, Jeon J, Jin Y, et al. Highly efficient gene knockout in mice and zebrafish with RNA-guided endonucleases. Genome Res 2014;24:125–31.
[32] Gong Z, Kennedy O, Sun H, Wu Y, Williams GA, Klein L, et al. Reductions in serum IGF-1 during aging impair health span. Aging Cell 2014;13:408–18.
[33] François JC, Aïd S, Chaker Z, Lacube P, Xu J, Fayad R, et al. Disrupting IGF signaling in adult mice conditions leanness, resilient energy metabolism, and high growth hormone pulses. Endocrinology 2017;158:2269–83.
[34] Blackburn A, Schmitt A, Schmidt P, Wanke R, Hermanns W, Brem G, et al. Actions and interactions of growth hormone and insulin-like growth factor-II: body and organ growth of transgenic mice. Transgenic Res 1997;6:213–22.
[35] Li M, Chen L, Tian S, Lin Y, Tang Q, Zhou X, et al. Comprehensive variation discovery and recovery of missing sequence in the pig genome using multiple de novo assemblies. Genome Res 2017;27:865–74.
[36] Yue F, Cheng Y, Breschi A, Vierstra J, Wu W, Ryba T, et al. Mouse ENCODE Consortium. A comparative encyclopedia of DNA elements in the mouse genome. Nature 2014;515:355–64.
[37] Matsuno K, Mae SI, Okada C, Nakamura M, Watanabe A, Toyoda T, et al. Redefining definitive endoderm subtypes by robust induction of human induced pluripotent stem cells. induced pluripotent stem cells. Differentiation 2016;92:281–90.
[38] Prummel KD, Nieuwenhuize S, Mosimann C. The lateral plate mesoderm. Development 2020;147:dev175059.
[39] Holzenberger M, Hamard G, Zaoui R, Leneuve P, Ducos B, Beccavin C, et al. Experimental IGF-I receptor deficiency generates a sexually dimorphic pattern of organ-specific growth deficits in mice, affecting fat tissue in particular. Endocrinology 2001;142:4469–78.
[40] Kruis T, Klammt J, Galli-Tsinopoulou A, Wallborn T, Schlicke M, Müller E, et al. Heterozygous mutation within a kinase-conserved motif of the insulin-like growth factor I receptor causes intrauterine and postnatal growth retardation. J Clin Endocrinol Metab 2010;95:1137–42.
[41] Walenkamp MJ, de Muinck Keizer-Schrama SM, de Mos M, Kalf ME, van Duyvenvoorde HA, Boot AM, et al. Successful long-term growth hormone therapy in a girl with haploinsufficiency of the insulin-like growth factor-I receptor due to a terminal 15q26.2->qter deletion detected by multiplex ligation probe amplification. J Clin Endocrinol Metab 2008;93:2421–5.
[42] Nagai T, Shimokawa O, Harada N, Sakazume S, Ohashi H, Matsumoto N, et al. Postnatal overgrowth by 15q-trisomy and intrauterine growth retardation by 15q-monosomy due to familial translocation t(13;15): dosage effect of IGF1R -? Am J Med Genet 2002;113:173–7.
[43] Roback EW, Barakat AJ, Dev VG, Mbikay M, Chrétien M, Butler MG. An infant with deletion of the distal long arm of chromosome 15 (q26.1––qter) and loss of insulin-like growth factor 1 receptor gene. Am J Med Genet 1991;38:74–9.